Current Eye Research, 35(7), 631–643, 2010

ISSN: 0271-3683 print/ 1460-2202 online
DOI: 10.3109/02713681003682925

informa
healthcare

ORIGINAL ARTICLE

Brief Exposure to Damaging Light Causes Focal Recruitment of Macrophages, and Long-Term Destabilization of Photoreceptors in the Albino Rat Retina

Matt Rutar[1,2], Jan M. Provis[1–3], and Krisztina Valter[1,2]

[1]*Research School of Biology, The Australian National University, Canberra ACT 0200, Australia*
[2]*ARC Centre of Excellence in Vision Science, The Australian National University, Canberra ACT 0200, Australia*
[3]*ANU Medical School, The Australian National University, Canberra ACT 0200, Australia*

ABSTRACT

Purpose: To characterize the long-term spatiotemporal features of light-mediated retinal degeneration.

Methods: Sprague–Dawley rats were exposed to 1000 lux for 24 h, then kept in dim light (5 lux), for up to 56 days. Animals were killed at 0, 3, 7, 28, and 56 days post-exposure, and retinas were prepared for immunohistochemistry. Outer nuclear layer (ONL) thickness and TUNEL labeling were used to quantify photoreceptor death. Antibodies to opsins, glial fibrillary acidic protein (GFAP), fibroblast growth factor-2 (FGF-2), and ED1 were used to assess the retina.

Results: At 0 days post-exposure, we detected photoreceptor death 2 mm superior to the optic disc (the "hotspot"), and ED1-positive macrophages in the retinal vasculature and underlying choroid. By 3 days, the ONL was thinner and there was gliosis in the outer retina, where ED1 positive macrophages were also present. Few ED1 positive cells remained at 28 days. At 56 days, there were TUNEL-positive nuclei in the penumbra, and increased FGF-2, and GFAP expression by Müller cells (MCs). In inferior retina, outer segment length was initially reduced, but recovered to near-normal by 28 days.

Conclusions: Short exposure to damaging light destabilizes the retina adjacent to a hotspot of degeneration, so that the damaged region expands in size over time. Recruitment of macrophages is associated with the early phase of damage, but not with the longer term photoreceptor loss in the penumbra. Features of the focal and progressive retinal damage in this model are reminiscent of the progression of age-related macular degeneration (AMD).

KEYWORDS: Age-related macular degeneration; Blood–retinal barrier; Light damage; Macrophages; Photoreceptor dystrophy; Retina

INTRODUCTION

Exposure to light of a sufficient intensity and duration has been shown to cause damage in the outer retina, particularly in the photoreceptor population.[1] In these models, photoreceptors die by apoptosis[2,3] primarily through a mechanism thought to involve oxidative damage.[4,5] In rat models of light-induced photoreceptor degeneration,[6] the region of retina superior to the optic disc is particularly susceptible to light-induced photoreceptor cell death,[7–9] the main area of damage being localized predominately to the temporal side.[10,11]

Received 16 September 2009; accepted 05 February 2010

Correspondence: Matt Rutar, Research School of Biology, The Australian National University, Canberra ACT 0200, Australia. E-mail: matt.rutar@rsbs.anu.edu.au

The spatial coincidence of this highly sensitive region with a local area where rod outer segments (OSs) are longer[12–14] and ganglion cell density is higher[15,16] suggests that the sensitive area is at the *area centralis*.[14]

There is extensive literature describing the histopathology associated with the rodent light-damage model, including photoreceptor cell death and dysfunction, and associated degeneration of the blood–retinal barrier (BRB).[1,17–21] However, the systematic progression and localization of retinal changes that follow a single photic insult, and its implications on the long-term stability of the surrounding retina have not been well characterized. In this study, we show that a relatively short exposure to bright continuous light (BCL) invokes localized, rapid changes in the outer retina of albino rats such that the initial focal damage leads to long-term destabilization of photoreceptors in the adjacent retina, so that the damaged region increases in size, over time. We suggest that the focal damage in the visual center of the albino rat retina is reminiscent of the histopathology of age-related macular degeneration (AMD).

METHODS

Animals and Light Exposure

All experiments conducted were in accordance with the ARVO Statement for the Use of Animals in Ophthalmic and Vision Research. Albino Sprague–Dawley (SD) rats were born and reared in dim cyclic light conditions (12 h light:12 h dark) with an ambient light level of approximately 5 lux. Exposure to BCL was conducted on animals aged between post-natal days (P) 90–150. Prior to BCL exposure, rats were dark adapted for a minimum of 15 h then transferred to individual cages designed to allow light to enter unimpeded. There were no areas of shadow in the cages; pupillary dilation was not performed. BCL exposure commenced consistently at 9:00 AM, and was achieved using a cold-white fluorescent light source positioned above the cages (18W, Cool White; TFC), at an intensity of approximately 1000 lux at the cage floor. BCL exposure was maintained over a period of 24 h, after which time the animals were immediately returned to dim cyclic conditions for the post-exposure period. Animals were kept in dim light conditions following BCL exposure for a maximum period of 56 days. Retinal tissue was analyzed from animals at the end of 24 h exposure and at 3, 7, 28, and 56 days. Age-matched, dim-reared animals served as controls.

Tissue Collection and Processing

Animals were killed by overdose of barbiturate administered through an intraperitoneal injection (60 mg/ kg body weight, Valabarb; Virbac, NSW, Australia). The left eye from each animal was marked at the superior surface for orientation then enucleated and processed for cryosectioning. Eyes were immediately immersion fixed in 4% paraformaldehyde in 0.1M phosphate-buffered solution (PBS) (pH 7.3) for 3 h at room temperature, then washed in 0.1M PBS before being left in a 15% sucrose solution overnight for cyroprotection. Eyes were oriented and embedded in O.C.T. compound (Tissue-Tek, Sakura, Japan) then snap frozen in liquid nitrogen and cryosectioned at 16 µm. The sections were mounted on gelatin/poly-L-lysine-coated glass slides coated and dried overnight at 50°C. Sections were stained for histological examination using hemotoxylin and eosin (H&E), or labeled using either immunohistochemistry or TUNEL.

The right eye from a minimum of three animals at each time-point was fixed in 2.5% glutaraldehyde, 2% paraformaldehyde in 0.1 M Cacodylate buffer (pH 7.4) for at least 6 h at room temperature and embedded for paraffin sectioning at 7 µm using a microtome. Sections were stained with cresyl violet and used to quantify photoreceptor OS length.

Analysis of Cell Death

TUNEL staining was used to quantify photoreceptor apoptosis following BCL in frozen sections using a protocol published previously.[22] Counts of TUNEL positive cells in the outer nuclear layer (ONL) were carried out along the full-length of retinal sections cut in the para-sagittal plane (superoinferior), including the optic disc, in adjacent fields measuring 1000 µm × 1000 µm. The final count from each animal is the average at comparable locations in two non-sequential sections. Statistical analysis was performed using a two-tailed Student's *t*-test. Differences with a P value < 0.05 were considered statistically significant. Thickness of the ONL in these sections was also measured in 1 mm intervals on the same sections. The DNA-specific dye Bisbenzamide (Calbiochem, La Jolla, California, USA) was used to visualize the cellular layers. ONL thickness was calculated as the ratio of ONL thickness to the distance between the outer- and inner-limiting membranes (OLMs and ILMs), to take into account any obliquely cut sections or regions. Statistical analysis was performed using a two-tailed Student's *t*-test.

OS Measurements

Analysis of photoreceptor OS length was performed on paraffin-embedded sections stained with cresyl violet. For each eye, images of four specific regions in the inferior and far-superior retina were acquired with an Axiocam MRc5 digital camera (Zeiss, NSW, Australia). From each of these images, four equi-spaced measurements of OS length were performed using AxioVision software (Version 4.2; Zeiss), which were averaged for each group of animals. Statistical analysis was performed using a two-tailed Student's *t*-test.

Immunohistochemistry

Sections adjacent to those used for TUNEL analysis were used for immunohistochemistry. Details for the antibodies used are displayed in Table 1. Sections were incubated in 10% normal goat serum (Sigma, St. Louis, MO, USA) for 1 h to block non-specific binding, before incubation in the primary antibody overnight at 4°C. Sections were washed in 0.1M PBS, then incubated in the appropriate secondary antibody overnight at 4°C (1:1000 anti-mouse IgG-alexa 594 or anti-rabbit IgG-alexa 488; Molecular Probes, Eugene, OR, USA). Sections were washed in 0.1M PBS then incubated in Bisbenzamide (1:1000) for 2 min and coverslipped in a glycerol/gelatin mixture. Primary antibodies were omitted to control for non-specific binding of the secondary antibody. Immunofluorescence was viewed using a Zeiss laser scanning microscope, and acquired using PASCAL software (Zeiss, v4.0). Images were enhanced for publication using Adobe Photoshop software, which was standardized between images.

TABLE 1 Antibodies used

Antibody	Dilution	Source
rabbit α L/M opsin	1:1000	Chemicon, Temecula, CA
mouse α rhodopsin (4D1)	1:500	Chemicon, Temecula, CA
rabbit α GFAP	1:700	Dako, Carpinteria, CA
mouse α FGF-2	1:100	Upstate, Temecula, CA
mouse α ED1	1:200	Chemicon, Temecula, CA
mouse α glutamine synthetase	1:1000	Chemicon, Temecula, CA

RESULTS

The Early Phase Post-Exposure: Emergence of a "Hotspot" of Degeneration

Following exposure to 24 h BCL, an increase in apoptotic profiles was evident along the vertical meridian of the ONL (Figure 1A), consistent with previous findings. The distribution of dying cells was not uniform along the retina. Rather, a circumscribed area approximately 2 mm supero-temporal to the optic disc was observed where TUNEL-positive (+) nuclei were concentrated. This "hotspot" appeared in the same location in all retinas examined, immediately following BCL. After 3 and 7 days post-exposure, the number of TUNEL+ nuclei had decreased substantially, but of those TUNEL+ cells detected, most were located in the hotspot or the immediately surrounding area.

Evidence of the cumulative impact of cell death on the photoreceptor population was demonstrated by differential changes in ONL thickness in the hotspot compared with other locations (Figure 1C). ONL thickness within the hotspot decreased rapidly so that by 3 days post-exposure, the ONL was 49.3% thinner than in controls ($P < 0.05$) at the center of the hotspot (2 mm eccentricity from the optic nerve). There was no further reduction in ONL thickness within the hotspot by 7 days post-exposure (51.7%; $P > 0.05$), consistent with the slowing of photoreceptor death over the course of the post-exposure period.

The structural and immunohistochemical changes that occur following light damage, at each time point, are shown in Figures 2 and 3. At 24 h post-exposure, only minor perturbations in retinal structure are evident compared with controls (Figure 2A), including evidence of minor disorganization in the inner portion of the ONL (Figure 2B; black arrow). At 3 and 7 days post-exposure, however, there are pronounced signs of stress and degeneration evident at the hotspot (Figures 2C, 2D and 3B). Thinning of the ONL at 3 days post-exposure is accompanied by accumulation of acellular debris in the layers that normally comprise photoreceptor OSs (Figure 2C and 2D). Surviving photoreceptors in the hotspot showed profound structural abnormalities from 3 days post-exposure, culminating in a virtual absence of rod and cone OSs by 7 days post-exposure (Figure 3A and 3B). This loss of photoreceptor OSs coincided with a redistribution of opsin into the soma and axon terminal by 7 days (Figure 3E, 3F, and 3G), highlighting structural abnormalities in the soma and axon.

We also observed interruption of the retinal pigment epithelium (RPE) monolayer by 3 days post-exposure (Figure 2C; black arrowhead), associated with debris-like deposits (Figure 2C; asterisks) and discontinuities in Bruch's membrane (Figure 2C; white arrow). Such disruption was also associated with an infiltration of large cells into the subretinal space (Figure 2D; black arrows). By 7 days post-exposure (Figure 2E), the

subretinal space was indistinct, so that the remains of the ONL abutted the choroid.

The emergence of major pathological features in the hotspot 3 days following BCL coincided with the formation of a "stress margin," or "penumbra," around the degenerating hotspot (Figure 2F). In the penumbra, there were pockets of hotspot-like degeneration (Figure 2F; black arrows) interspersed with regions of

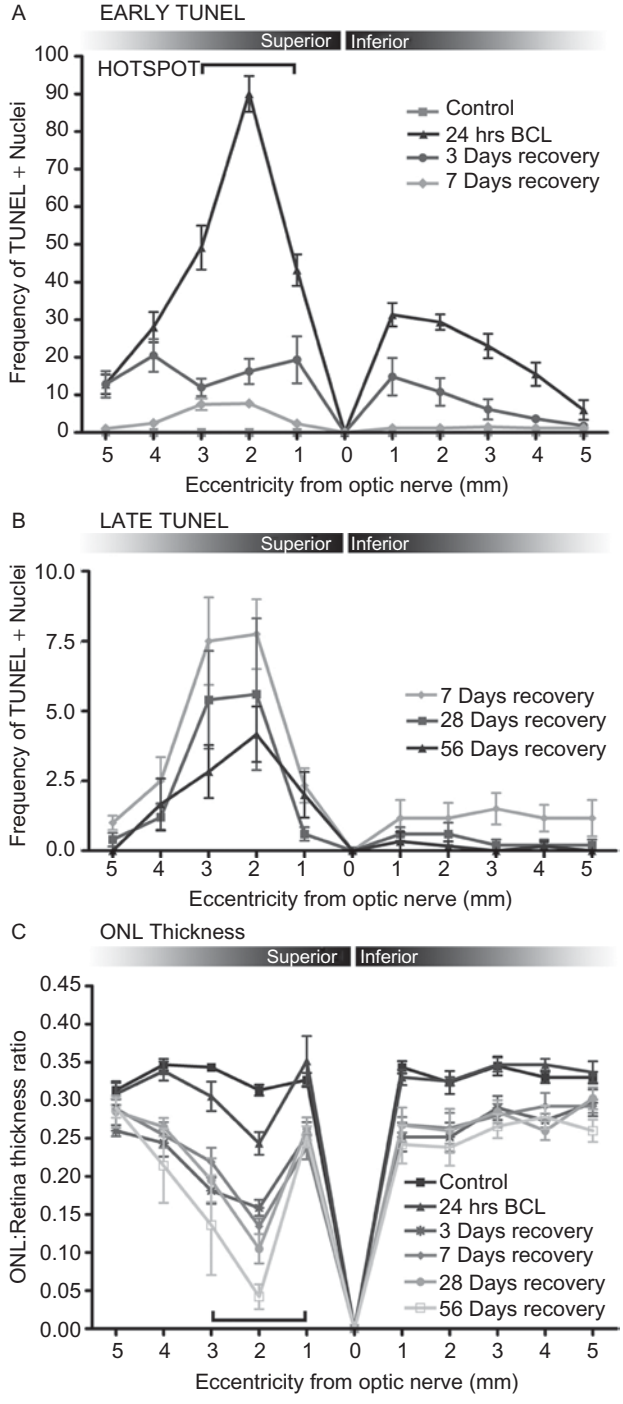

FIGURE 1 Distribution of photoreceptor cell death in the ONL following exposure to BCL. (A) TUNEL+ cell counts over the length of the retina immediately following BCL reveal a dense localization of TUNEL+ nuclei to a hotspot in the superior retina approximately 2 mm from the optic nerve. The number of TUNEL+ cells diminishes following 3 days post-exposure, but remains persistent at a low level within the hotspot after 7 days. (Control $n = 6$; 0 days $n = 6$; 3 days $n = 6$; 7 days $n = 6$; error bars represent SEM.) (B) Chronic appearance of TUNEL+ nuclei is shown to cluster within and around the hotspot from 7 days post-exposure onward. (7 Days $n = 6$; 28 days $n = 5$; 56 days $n = 6$; error bars represent SEM.) (C) ONL thickness measurements across the retina illustrate an emerging depression in ONL thickness developing rapidly after 3 days post-exposure. (Control $n = 6$; 0 days $n = 6$; 3 days $n = 8$; 7 days $n = 9$; 28 days $n = 4$; 56 days $n = 5$; error bars represent SEM.) BCL, bright continuous light; ONL, outer nuclear layer.

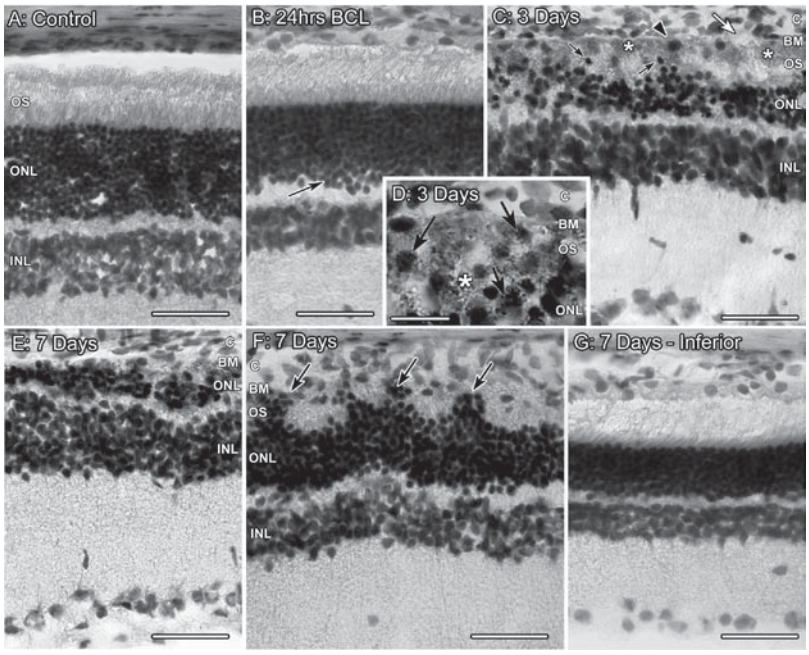

FIGURE 2 Histological examination using H&E staining of the emerging pathology of the hotspot during 0–7 days post-BCL exposure. (A) Retinal section of a dim-reared young-adult rat from the superior mid-periphery. (B) Section from the hotspot of TUNEL+ cell death immediately after 24 h BCL, showing a slight destabilization of the inner portion of the ONL (arrow). (C) After 3 days recovery, a vast disruption in the integrity of the outer retina is depicted, including gross disorganization of the ONL (black arrows), and accumulations of debris (asterisks). The RPE is disrupted amongst clumps of debris (black arrowhead), and Bruch's membrane appeared discontinuous in parts (white arrow). (D) High magnification of a section of the hotspot after 3 days post-exposure reveal large nuclei (arrows) within the subretinal space and ONL in addition to considerable debris (white asterisk). (E) Sections from 7 days post-exposure depict the progressive formation of the retinal lesion with the collapse of ONL into the subretinal space, with pockets of debris still apparent. (F) Intermediate manifestations of retinal disruption toward the edge of the hotspot after 7 days post-exposure. Rosette structures within the ONL are formed as isolated regions collapse into the OS layer (arrows). (G) A region from the inferior mid-periphery 7-day post-exposure representing the maintenance of structural integrity outside the hotspot. BCL, bright continuous light; BM, Bruch's membrane; C, choroidal vasculature; H&E, hemotoxylin and eosin; INL, inner nuclear layer; ONL, outer nuclear layer; OSs, outer segments; RPE, retinal pigment epithelium; S, subretinal space. Scale bars represent 50 µm (A–C, E–G) and 20 µm (D).

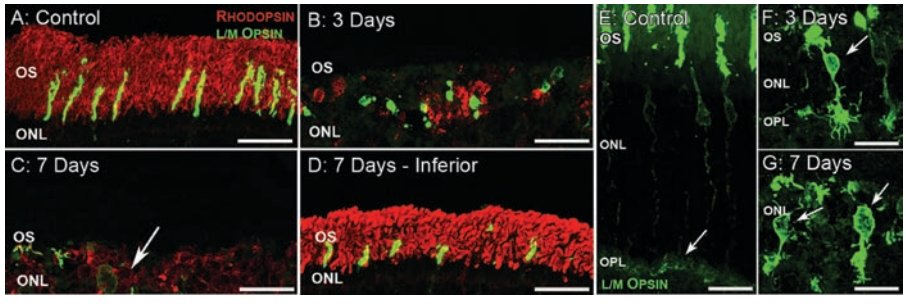

FIGURE 3 Changes in photoreceptor morphology within the hotspot following exposure to BCL. Sections are immunolabeled with L/M opsin (green) and Rhodopsin (red) in A–D. E–G depict high gain and magnification of photoreceptor cell bodies, illustrating BCL-induced changes in L/M opsin (green) distribution beyond the OSs. (A) Photoreceptors from a dim-reared animal showing slender, organized OSs. (B) Retinal section of the hotspot after 3 days recovery showing extreme reduction of OSs in both rods and cones to small disorganized fragments dotting the OS layer. (C) Seven days post-exposure section revealing OSs nearly absent among photoreceptors in the hotspot, with immunoreactivity for L/M opsin and rhodopsin becoming redistributed to within the somas of the photoreceptors (arrow). (D) Shortening of OSs is shown in the inferior retina after 7 days; however, structural integrity is maintained. (E–G) L/M opsin immunoreactivity in the hotspot after 3- and 7-day post-exposure respectively; (F and G). An increased distribution of photopigment from the OSs to soma and axon terminals in some photoreceptors (arrows) in contrast to controls (E). The redistribution also reveals the distorted structure of surviving photoreceptors. BCL, bright continuous light; INL, inner nuclear layer; IPL, inner plexiform layer; ONL, outer nuclear layer; OPL, outer plexiform layer; OSs, outer segments. Scale bars represent 50 µm (A–D) and 20 µm (E–G).

relatively normal appearance, where photoreceptor OSs were still present and giving rise to rosette-like formations in the outer retina. Beyond the penumbra, although there was pronounced thinning of the ONL, the retina and Bruch's membrane appeared to be structurally intact (Figure 2G).

Localized changes in Müller cells (MCs) were also evident following BCL (Figure 4). Changes in immunoreactivity for glial fibrillary acidic protein (GFAP) were apparent within inner MC processes in the hotspot immediately following BCL exposure (Figure 4B; arrow), in contrast to typical expression predominately within the astrocytes (Figure 4A). By 3 days post-exposure and at 7 days post-exposure, GFAP immunoreactivity was intense in the inner and outer MC processes (Figure 4C and 4D; white arrowheads). This extensive labeling coincided with profound structural rearrangement suggestive of reactive gliosis within the hotspot (Figure 4H and 4I). Labeling of MCs using anti-glutamine synthetase—a known MC marker[23]—showed hypertrophied MC processes in the remnant ONL at 3 and 7 days post-exposure (Figure 4H and 4I; white asterisks), which infiltrated the subretinal space to form a mass of processes (white arrows), suggestive of a fibroglial scar. Despite sustaining substantial visual cell loss, regions of retina in the inferior showed intact MC morphology and OLM integrity at 7 days post-BCL exposure (Figure 4J), with GFAP expression also comparatively attenuated in the outer processes (Figure 4E).

Recruitment of ED1-Positive Macrophages to the Hotspot

During the early phase post-exposure to BCL, we found evidence of macrophage recruitment into the hotspot, evidenced by ED1 immunoreactivity—a known marker for rat macrophages[24] (Figure 5). A preferential clustering of ED1-positive cells was apparent in the choroidal vasculature underlying the hotspot, immediately following BCL exposure (Figure 5B). This recruitment was localized to the hotspot, with virtually no ED1-positive nuclei observed in the choroid outside the hotspot (Figure 5C). Numerous ED1-positive cells were also observed in the retinal blood vessels immediately after BCL exposure (Figure 5D). By 3 days post-BCL exposure, ED1-macrophages were present among the degenerating remains of the OSs and in the ONL (Figure 5E; arrows). ED1-positive nuclei in both the ONL and vasculature was largely dissipated by 28 days post-exposure, reaching num-

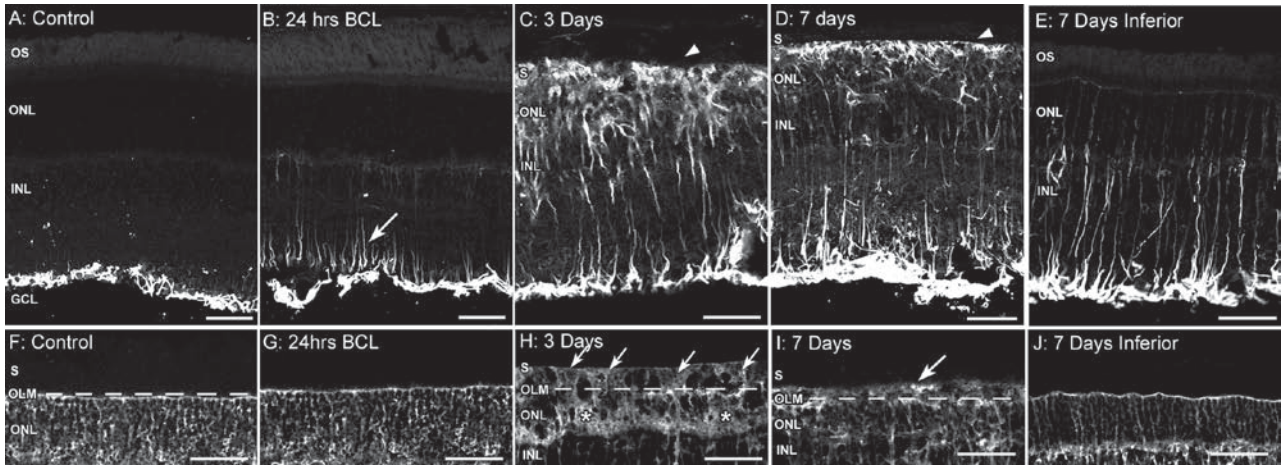

FIGURE 4 GFAP expression and reactive gliosis of Müller cells (MCs) in the hotspot during the early post-exposure period. Sections are immunolabeled with GFAP in A–E, and with glutamine synthetase to visualize MC morphology in F–J. (A) Typical retinal GFAP expression in the superior mid-periphery from a dim-reared animal. (B) Immunoreactivity for GFAP becomes evident in the inner processes of the MCs (arrow) immediately following exposure to BCL. (C and D) GFAP immunoreactivity features heavily throughout the MC in the hotspot at both 3 and 7 days post-exposure, localizing particularly within the rapidly formed glial scar situated below the ONL (white arrowheads). (E) Upregulation of GFAP is also evident outside the hotspot in the inferior mid-periphery at 7 days post-exposure, although expression is mainly limited to the inner MC processes. (F) Retinal section from a dim-reared animal immunolabeled with glutamine synthetase showing normal MC morphology; a dashed line marks the outer limiting membrane. (G) The structural integrity of the OLM is maintained in the hotspot immediately following exposure to BCL. (H) Sections from 3 days post-exposure show reactive gliosis apparent within the hotspot. The integrity of the OLM is disturbed as MC processes hypertrophy (asterisks) and infiltrate the subretinal space, forming a fibroglial scar beyond the subretinal space (arrows). (I) MC processes continue to infiltrate into the subretinal space after 7-day post-exposure. (J) A retinal section from the inferior mid-periphery demonstrates the retention of OLM integrity outside the hotspot. BCL, bright continuous light; C, choroidal vasculature; GCL, ganglion cell layer; GFAP, glial fibrillary acidic protein; INL, inner nuclear layer; OLM, outer limiting membrane; ONL, outer nuclear layer; OSs, outer segments. Scale bars represent 50 μm (A–J).

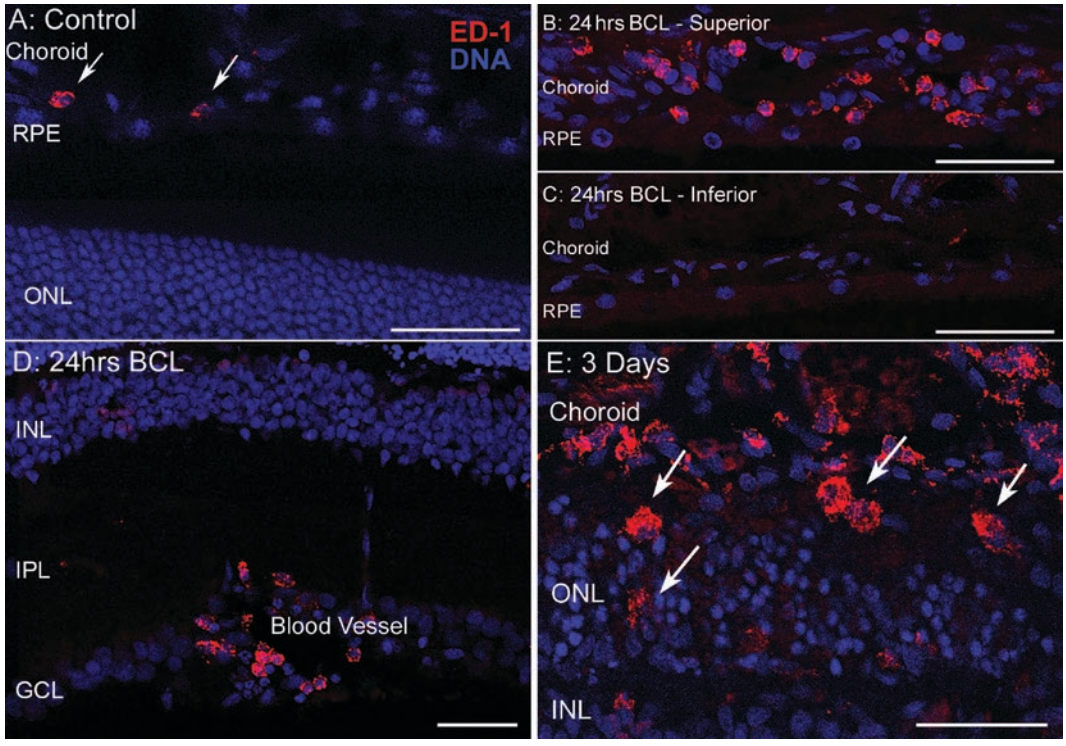

FIGURE 5 Preferential recruitment of ED1-positive macrophages to the hotspot following exposure to BCL. Sections are immunolabeled with ED1 for rat macrophages (red) and for nuclei as labeled with bisbenzamide (blue) in A–E. (A) ED1-postive nuclei are rare and sparsely localized within the choroidal vasculature of dim-reared animals (arrows). B and C: Sections immediately following BCL show a marked recruitment of ED1-macrophages to the choroidal vasculature underlying the hotspot (B), while showing no such localization to non-hotspot retina (inferior mid-periphery) (C). (D) Incursion of ED1-positive nuclei into the superficial retinal vasculature is highly evident in association with the hotspot, immediately following BCL. (E) Retinal section at 3 days post-exposure showing ED1-positive macrophages present in the subretinal space and ONL within the hotspot (arrows). C, choroidal vasculature; GCL, ganglion cell layer; INL, inner nuclear layer; IPL, inner plexiform layer; ONL, outer nuclear layer; RPE, retinal pigment epithelium. Scale bars represent 50 μm (A–E).

bers similar to controls by 56-day post-exposure (data not shown).

The Late Phase Post-Exposure: Persistence of Degeneration Around the Hotspot

The stability of BCL-exposed retinas was also assessed at 28- and 56-day post-exposure. TUNEL cell counts in the ONL across the vertical meridian of retinas 28 days following BCL exposure show persistence of TUNEL+ nuclei in a broad region in and around the hotspot even at 56 days post-BCL exposure (Figure 1B). A cumulative impact of this chronic photoreceptor loss was observed through the persistent decrease in ONL thickness associated with the hotspot. By 56 days post-exposure, the relative reduction in ONL thickness compared with dim-reared animals (86.6%) was found to have increased by 34.9% ($P < 0.05$) over measurements taken after 7 days post-exposure (51.7%) at comparable locations in the hotspot (2 mm superior from the optic nerve).

Histologically, at 28 and 56 days post-exposure, only a few scattered photoreceptors were present in the ONL, which appeared compressed between the choroid and INL (Figure 6A and 6B). In contrast, structural integrity was maintained in the inferior retina as late as 56 days post-exposure. Immunoreactivity for L/M opsin and rhodopsin revealed a sparse population of surviving photoreceptors in the hotspot, mainly comprising disorganized cones, with rods present only toward the rim of the hotspot (Figure 6H and 6I). The remaining cones had lost their normally slender, elongated morphology, lacked inner and OSs and were immunoreactive to L/M opsin throughout the soma and axon terminals (Figure 6I). On the edge of the lesion, there was marked upregulation of GFAP expression by MC (Figure 6C and 6G), increased immunoreactivity for fibroblast growth factor-2 (FGF-2) in photoreceptor nuclei (Figure 6E and 6F), and the continued presence of TUNEL+ nuclei (Figure 6G) indicative of continued photoreceptor loss on the edge of the hotspot, long after BCL exposure.

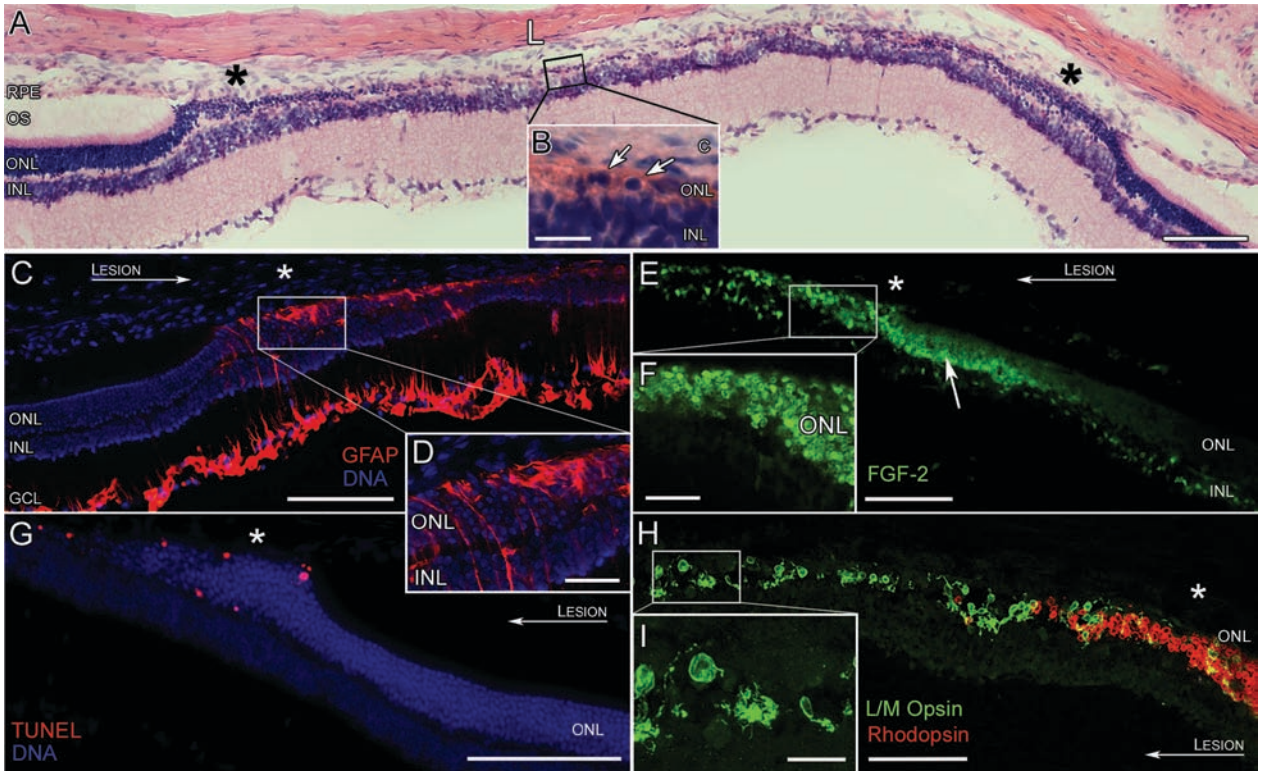

FIGURE 6 Instability and degeneration among photoreceptors in-and-surrounding the hotspot at 56-day post-exposure. (A and B) H&E stained sections of a hotspot lesion (L) 56 days after BCL exposure show further reduction in ONL to a mere few degenerative nuclei compacted within the scar tissue of the retinal lesion (B; arrows). A substantial cluster of degenerative photoreceptors is apparent in the penumbra (black asterisks), in which nuclei appear disorganized while lacking inner and outer segments. (C and D) Immunoreactivity for GFAP (red) shows heavy localization to the outer processes of Müller cells within the cluster of photoreceptor nuclei on the edge (asterisk) of the hotspot as visualized with bisbenzamide (blue). (E and F) From the penumbra (asterisk), photoreceptor nuclei display preferential labeling (arrow) for the neuroprotective factor FGF-2 (green), which recedes with increasing distance from the lesion. (G) TUNEL+ nuclei (red) clustering on the edge of the hotspot (asterisk) at 56 days post-exposure, the blue label is bisbenzamide. (H–I) Immunoreactivity for rhodopsin (red) and L/M opsin (green) in the hotspot at 56 days post-exposure. Photoreceptors are mainly composed of L/M opsin immunoreactive cone remnants (I) toward the center of the lesion, while degenerative OS-lacking rods predominate from the rim of the hotspot (asterisk) (H). GCL, ganglion cell layer; H&E, hemotoxylin and eosin; INL, inner nuclear layer; IPL, inner plexiform layer; ONL, outer nuclear layer; OSs, outer segments; RPE, retinal pigment epithelium. Scale bars represent 100 μm (A, C, E, G, H), and 20 μm (B, D, F, I).

Recovery of Photoreceptors Outside the Hotspot

Contrasting with the sustained degeneration of photoreceptors associated with the hotspot, we found evidence of photoreceptor recovery in the inferior and far-superior retina following photic insult (Figure 7). Measurement of photoreceptor OSs in these regions following BCL showed a shortening of OSs to 57% the length of dim-reared controls by 7 days post-exposure ($P < 0.05$; Figure 7A), whereas immunoreactivity for L/M opsin displayed a heavy translocation to the soma and axon (Figure 7C). However, by 28 days post-exposure OS length had recovered to approximately 90% the length of controls at comparable locations ($P < 0.05$), which was maintained after 56 days post-exposure (Figure 7A). Recovery of OS length at this time was also associated with a reduction in L/M opsin immunoreactivity in the soma and axonal processes of cones, with opsin immunoreactivity confined predominately to the OSs (Figure 7D).

DISCUSSION

The results of this study confirm in this model the highly focal nature of light-induced photoreceptor degeneration in a "hotspot," as described previously,[10] and further emphasize its co-localization with the *area centralis* of the rat retina.[14] In addition, our findings elaborate on the existing understanding of this light-induced model of retinal degeneration in that we show (i) that photoreceptor degeneration continues in the hotspot and surrounding *penumbra* up to 56 days post-exposure, resulting in expansion of the hotspot, while (ii) photoreceptors in inferior and

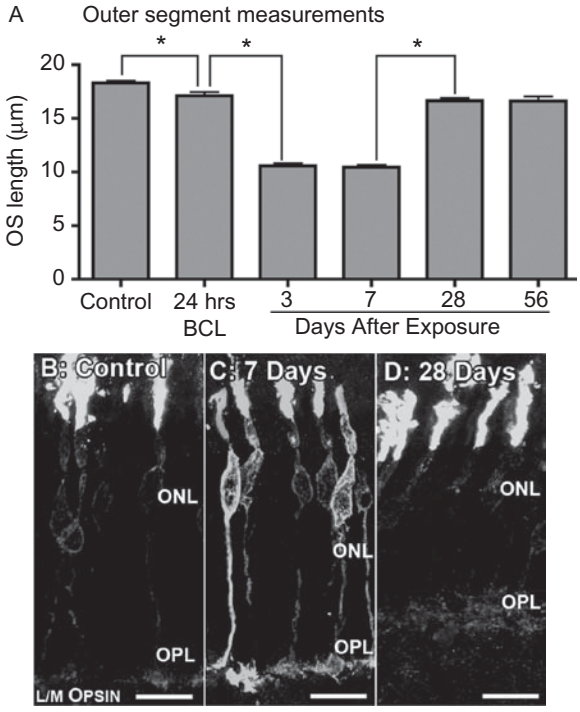

FIGURE 7 Long-term recovery of photoreceptor morphology in non-hotspot regions of retina. (A) Quantitative measurements of OS length from consistent populations of photoreceptors in the inferior and far-superior show a vast reduction in OS length after 3 days post-exposure. A significant renewal of OSs, however, is demonstrated at 28 days post-exposure (Control $n=8$; 0 days $n=6$; 3 days $n=3$; 7 days $n=4$; 28 days $n=4$; 56 days $n=5$; error bars represent SEM; "*" denotes a significant change where $P<0.05$). (B–D) Sections immunolabeled with L/M opsin reveal a strong redistribution of L/M opsin to the soma and axon in some cones within the inferior mid-periphery 7 days after BCL exposure (C) compared to controls (B). At 28 days recovery, L/M opsin labeling shows a normal distribution (D). ONL, outer nuclear layer; OPL, outer plexiform layer; OSs, outer segments. Scale bars represent 20 μm (B–D).

far superior retina show substantial recovery from photic insult between 7 and 28 days post-exposure. We also demonstrate (iii) localized recruitment of ED1-positive macrophages to the choroid underlying the hotspot, and in the inner retinal vasculature near the hotspot which is evident 24 h from commencement of bright light exposure, and (iv) infiltration of the outer retina by ED1-positive macrophages by 3 days post-exposure, associated with breakdown of the outer BRB, and the elaboration of MC processes in the subretinal space.

To our knowledge, the spatiotemporal relationship of these characteristics following light damage to the retina in the albino rat has not been explored previously. Our findings are consistent with earlier reports showing that in the albino rat retina 24 h exposure to BCL invokes localized, rapid changes in the outer retina that result in photoreceptor death by apoptosis. In addition, we show that the hotspot—the region most affected in the short term—is surrounded by a *penumbra* where photoreceptor death continues at levels substantially higher than background, until at least 56 days post-exposure. Persistent photoreceptor death and stress in the penumbra results in a gradual increase in the size of the hotspot over this period, consistent with observations from another phototoxic model, using Lister hooded and RCS rats.[11] We also find death of rod photoreceptors ahead of cone photoreceptors, and persistence of opsin-expressing cone somata within the degenerating region at 56 days. In contrast, we find that, remote from the hotspot in far-superior and in inferior retina, there is evidence of recovery from light damage over the 56-day period, demonstrated by the recovery of near-normal OS length in photoreceptors in these regions.[17,25–27] Together our findings indicate that there are region-specific factors that predispose the more central regions of the albino rat retina to the prolonged effects of retinal damage, which are not in effect in inferior and far-superior retinal locations.

The regional nature of photoreceptor cell death in this model has been well documented; however, the notion that the hotspot of degeneration may result from specializations associated with the *area centralis* has received relatively little attention. Specializations of the rat *area centralis*, which may render this region more susceptible to light-induced degeneration, have been alluded previously.[14] At the *area centralis*, the OSs are more elongated and have higher rhodopsin content,[12,14,28] and other studies show a correlation between rhodopsin content and the severity of light damage.[8,28,29] One possibility is that regional responses of the retina to light damage over the 56-day period may be due to the relative severity of the initial photic insult on the retina in the different regions, the *area centralis* being more severely affected due to local photoreceptor specializations. However, further studies that include controls for rhodopsin content are required to specifically address this hypothesis.

We also detected region-specific recruitment of activated macrophages to the incipient hotspot, early in the post-exposure period. Recruitment of macrophages in light-damage models of retinal degeneration has been shown previously, albeit in a more delayed fashion. Gordon and colleagues (2002) showed that 4–5 h exposure to high intensity white light (1800 lux) resulted in DNA fragmentation that was associated with monocyte recruitment into the ONL by 42 h post-treatment.[30] Similarly, in a high-intensity model utilizing blue light, ED1-positive macrophages were detected in the ONL 7 days after exposure to damaging light.[31] Activated microglia have also been implicated in progression of photoreceptor degeneration in a light-induced model,[32] as well as in *rd* mice.[33] However, those studies did not

report detection of ED1-positive cells in the choroid, nor did they report regional variation in the recruitment of the activated cells. The present findings show early, site-specific recruitment of ED1-positive cells 24 h from commencement of bright light exposure, in both the choroidal and the retinal vascular supplies, in the region of the hotspot, but not elsewhere in the retina. By 3 days post-exposure, we found that many ED1-positive cells had migrated into the degenerating ONL of the hotspot, consistent with previous reports, and by 28 days post-exposure, the invasion of ED1-positive cells had largely abated. The precise role played by the ED1-positive macrophages in the progress of photoreceptor degeneration remains unclear. One interpretation is that macrophages are recruited to the site of retinal damage to facilitate clearance of cellular debris resulting from cell death,[24,34] However, it has also been shown that suppression of activation of the retina's resident macrophages, the microglia, significantly reduces photoreceptor death, suggesting that activated macrophages may have an active role in the progress of light-induced photoreceptor loss.[31] In support of this hypothesis, *in vitro* studies show increased levels of death among cultured photoreceptors exposed to basal medium conditioned by activated microglia.[35]

Comparison with AMD

The progress of retinal degeneration described here over the 56-day period post-exposure to damaging light bears many similarities with the progression of AMD in the absence of neovascularization, albeit in a considerably compressed timeframe.[36] First, photoreceptor loss in this model is strictly centered on the *area centralis*, a retinal specialization that is a homolog of the *fovea centralis*, and found predominantly in predatory and crepuscular mammals.[37] Both *foveae* and *areae centrales* are adapted to mediate best spatial resolution, and include a range of specializations, which in humans may predispose the *fovea* and surrounding *macula* to degeneration.[38,39] Second, loss of the RPE, [40] breaks in Bruch's membrane,[41–44] MC gliosis and GFAP upregulation,[45] and changes to the choroid [46–49] are all features of early AMD. Consistent with findings from previous light-damage studies,[36,50] we find a similar range of features emerging following exposure to BCL, albeit in different time frames, post-exposure.

The present findings also show new features of the light-damage model of retinal degeneration that support the analogy with AMD. First, the focal accumulation of ED1-positive macrophages to the choroid underlying the incipient hotspot following BCL bears striking similarity to the increased infiltration and activation of leukocytes characterized in the macular choroid in both early and late AMD.[42,51–54] Such accumulations of macrophages are known to be associated with the progression and severity of AMD histopathology. Studies involving experimental models of choroidal neovascularization have shown that macrophage inhibition induced through liposomal clodronate[55,56] or deficiency in the fractalkine chemokine receptor (CX3CR1)[57] reduces the resulting lesion size.

Second, our long-term analysis of photoreceptor death and immunoreactivity for stress-related proteins in MC shows the spread of a focal lesion into adjacent retina over time, resembling the expansion of retinal lesions in the "dry" form of AMD.[40,58,59] Third, the changes detected in photoreceptors in and around the emerging hotspot are similar to those seen in photoreceptors in and around AMD lesions.[60] These include an initial redistribution of opsin from the OSs to the soma and pedicles,[60–63] followed by hypertrophy of the soma and axon terminal in cones, then loss of OSs and axon terminals in cones in the center of the lesion, where islands of surviving cone somata can be detected.[60]

Two features of AMD not observed in the light damage model, however, are drusen and neovascularization. Although the precise origins and significance of drusen remain elusive, it is understood that they are complex deposits that form over a long period of time,[64] possibly in response to pro-inflammatory signals.[65] Furthermore, it has been suggested that C3a and C5a present in drusen may promote choroidal neovascularization in AMD.[66] We suggest, therefore, that the light-induced retinal degeneration seen in the albino rat model differs from AMD in that it develops over a very short time-frame, and the characteristics of AMD that develop long term—drusen and neovascularization—are not observed.

Light exposure has been associated with the incidence of AMD in a number of studies previously,[67–73] although the association has remained somewhat contentious[74–76] and may stem from the difficulty of accurately assessing a lifetime of light-exposure through questionnaires.[77,78] Indeed, a recent investigation by Hirakawa and colleagues (2008), which utilized an objective means to gauge light exposure, has also demonstrated a link between increased sunlight and AMD.[77] Several lines of evidence also support an association between the casual events both of AMD and light damage, specifically through oxidative damage. Light-induced oxidative damage has been shown to arise through rhodopsin-mediated peroxidation of lipids, such as docosahexanic acid (DHA),[4,5,79] and a role for oxidative damage has long been suggested in the pathogenesis of AMD.[80,81] This association has been further strengthened by recent findings implicating carboxyethylpyrrole (CEP)—an oxidation fragment of

DHA and biomarker of AMD[82–84]—in the emergence of AMD histopathology.[85]

CONCLUSIONS

Our findings show that a rapid and prolonged development of AMD-like histopathology occurs in albino rats exposed for a relatively short period of BCL, which features a strong localization to the apparent visual center of the rat retina. Building on previous findings,[36,50] our data offer compelling histological evidence for a common pathway underpinning the process of photoreceptor degeneration in this model of light damage and AMD, and show the potential of this model for analysis of mechanisms of retinal degeneration.

ACKNOWLEDGMENT

This work was supported by Australian Research Council Centres of Excellence Program (CE0561903); Ophthalmic Research Institute of Australia/Brenda Mitchell grant.

***Declaration of interest*:**The authors report no conflicts of interest. The authors alone are responsible for the content and writing of the paper.

REFERENCES

[1] Noell WK, Walker VS, Kang BS, Berman S. Retinal damage by light in rats. *Invest Ophthalmol* 1966;5:450–473.
[2] Abler AS, Chang CJ, Ful J, Tso MO, Lam TT. Photic injury triggers apoptosis of photoreceptor cells. *Res Commun Mol Pathol Pharmacol* 1996;92:177–189.
[3] Bowers F, Valter K, Chan S, et al. Effects of oxygen and bFGF on the vulnerability of photoreceptors to light damage. *Invest Ophthalmol Vis Sci* 2001;42:804–815.
[4] Demontis GC, Longoni B, Marchiafava PL. Molecular steps involved in light-induced oxidative damage to retinal rods. *Invest Ophthalmol Vis Sci* 2002;43:2421–2427.
[5] Wiegand RD, Giusto NM, Rapp LM, Anderson RE. Evidence for rod outer segment lipid peroxidation following constant illumination of the rat retina. *Invest Ophthalmol Vis Sci* 1983;24:1433–1435.
[6] Chader GJ. Animal models in research on retinal degenerations: past progress and future hope. *Vision Res* 2002;42: 393–399.
[7] Noell WK. Possible mechanisms of photoreceptor damage by light in mammalian eyes. *Vision Res* 1980;20:1163–1171.
[8] Rapp LM, Tolman BL, Koutz CA, Thum LA. Predisposing factors to light-induced photoreceptor cell damage: retinal changes in maturing rats. *Exp Eye Res* 1990;51: 177–184.
[9] Rapp LM, Smith SC. Morphologic comparisons between rhodopsin-mediated and short-wavelength classes of retinal light damage. *Invest Ophthalmol Vis Sci* 1992;33:3367–3377.
[10] Tanito M, Kaidzu S, Ohira A, Anderson RE. Topography of retinal damage in light-exposed albino rats. *Exp Eye Res* 2008;87:292–295.
[11] Marco-Gomariz MA, Hurtado-Montalbán N, Vidal-Sanz M, Lund RD, Villegas-Pérez MP. Phototoxic-induced photoreceptor degeneration causes retinal ganglion cell degeneration in pigmented rats. *J Comp Neurol* 2006;498:163–179.
[12] Battelle BA, LaVail MM. Rhodopsin content and rod outer segment length in albino rat eyes: modification by dark adaptation. *Exp Eye Res* 1978;26:487–497.
[13] Penn JS, Williams TP. Photostasis: regulation of daily photon-catch by rat retinas in response to various cyclic illuminances. *Exp Eye Res* 1986;43:915–928.
[14] Rapp L, Naash M, Wiegand R, et al. Morphological and biochemical comparisons between retinal regions having differing susceptibility to photoreceptor degeneration. In: LaVail MM, Hollyfield JG, Anderson RE (eds), Retinal Degeneration: Experimental and Clinical Studies: Liss Alan R Inc, 1985, pp. 421–437.
[15] Fukuda Y. A three-group classification of rat retinal ganglion cells: histological and physiological studies. *Brain Res* 1977;327–344.
[16] Carpenter P, Sefton AJ, Dreher B, Lim WL. Role of target tissue in regulating the development of retinal ganglion cells in the albino rat: effects of kainate lesions in the superior colliculus. *J Comp Neurol* 1986;251:240–259.
[17] Kuwabara T. Retinal recovery from exposure to light. *Am J Ophthalmol* 1970;70:187–198.
[18] Kuwabara T, Funahashi M. Light damage in the developing rat retina. *Arch Ophthalmol* 1976;94:1369–1374.
[19] Oraedu AC, Voaden MJ, Marshall J. Photochemical damage in the albino rat retina: morphological changes and endogenous amino acids. *J Neurochem* 1980;35:1361–1369.
[20] Hansson HR. A histochemical study of cellular reactions in the rat retina transiently damaged by visible light. *Exp Eye Res* 1971;12:270–274.
[21] van Best JA, Putting BJ, Oosterhuis JA, Zweypfenning RC, Vrensen GF. Function and morphology of the retinal pigment epithelium after light-induced damage. *Microsc Res Tech* 1997;36:77–88.
[22] Maslim J, Valter K, Egensperger R, Holländer H, Stone J. Tissue oxygen during a critical developmental period controls the death and survival of photoreceptors. *Invest Ophthalmol Vis Sci* 1997;38:1667–1677.
[23] Bringmann A, Pannicke T, Grosche J, et al. Mü,ller cells in the healthy and diseased retina. *Prog Retin Eye Res* 2006;25:397–424.
[24] Chen L, Yang P, Kijlstra A. Distribution, markers, and functions of retinal microglia. *Ocul Immunol Inflamm* 2002;10: 27–39.
[25] Moriya M, Baker BN, Williams TP. Progression and reversibility of early light-induced alterations in rat retinal rods. *Cell Tissue Res* 1986;246:607–621.
[26] Jozwick C, Valter K, Stone J. Reversal of functional loss in the P23H-3 rat retina by management of ambient light. *Exp Eye Res* 2006;83:1074–1080.
[27] Chrysostomou V, Stone J, Stowe S, Barnett NL, Valter K. The status of cones in the rhodopsin mutant P23H-3 retina: light-regulated damage and repair in parallel with rods. *Invest Ophthalmol Vis Sci* 2008;49:1116–1125.
[28] Rapp LM, Williams TP. Rhodopsin content and electroretinographic sensitivity in light-damaged rat retina. *Nature* 1977;267:835–836.
[29] Grimm C, Wenzel A, Hafezi F, et al. Protection of Rpe65-deficient mice identifies rhodopsin as a mediator of light-induced retinal degeneration. *Nat Genet* 2000;25:63–66.

[30] Gordon WC, Casey DM, Lukiw WJ, Bazan NG. DNA damage and repair in light-induced photoreceptor degeneration. *Invest Ophthalmol Vis Sci* 2002;43:3511–3521.
[31] Ni YQ, Xu GZ, Hu WZ, et al. Neuroprotective effects of naloxone against light-induced photoreceptor degeneration through inhibiting retinal microglial activation. *Invest Ophthalmol Vis Sci* 2008;49:2589–2598.
[32] Zhang C, Shen JK, Lam TT, et al. Activation of microglia and chemokines in light-induced retinal degeneration. *Mol Vis* 2005;11:887–895.
[33] Zeng HY, Zhu XA, Zhang C, et al. Identification of sequential events and factors associated with microglial activation, migration, and cytotoxicity in retinal degeneration in rd mice. *Invest Ophthalmol Vis Sci* 2005;46:2992–2999.
[34] Joly S, Francke M, Ulbricht E, et al. Cooperative phagocytes: resident microglia and bone marrow immigrants remove dead photoreceptors in retinal lesions. *Am J Pathol* 2009;174:2310–2323.
[35] Roque RS, Rosales AA, Jingjing L, Agarwal N, Al-Ubaidi MR. Retina-derived microglial cells induce photoreceptor cell death in vitro. *Brain Res* 1999;836:110–119.
[36] Marc RE, Jones BW, Watt CB, et al. Extreme retinal remodeling triggered by light damage: implications for age related macular degeneration. *Mol Vis* 2008;14:782–806.
[37] Rowe MH, Dreher B. Functional morphology of beta cells in the area centralis of the cat's retina: a model for the evolution of central retinal specializations. *Brain Behav Evol* 1982;21:1–23.
[38] Penfold PL, Madigan MC, Gillies MC, Provis JM. Immunological and aetiological aspects of macular degeneration. *Prog Retin Eye Res* 2001;20:385–414.
[39] Provis JM, Penfold PL, Cornish EE, Sandercoe TM, Madigan MC. Anatomy and development of the macula: specialisation and the vulnerability to macular degeneration. *Clin Exp Optom* 2005;88:269–281.
[40] Sarks JP, Sarks SH, Killingsworth MC. Evolution of geographic atrophy of the retinal pigment epithelium. *Eye (Lond)* 1988;2 (Pt 5):552–577.
[41] Penfold P, Killingsworth M, Sarks S. An ultrastructural study of the role of leucocytes and fibroblasts in the breakdown of Bruch's membrane. *Aust J Ophthalmol* 1984;12:23–31.
[42] Penfold PL, Killingsworth MC, Sarks SH. Senile macular degeneration. The involvement of giant cells in atrophy of the retinal pigment epithelium. *Invest Ophthalmol Vis Sci* 1986;27:364–371.
[43] Green WR. Histopathology of age-related macular degeneration. *Mol Vis* 1999;5:27.
[44] Green WR, Enger C. Age-related macular degeneration histopathologic studies. The 1992 Lorenz E. Zimmerman Lecture. *Ophthalmology* 1993;100:1519–1535.
[45] Wu KH, Madigan MC, Billson FA, Penfold PL. Differential expression of GFAP in early v late AMD: a quantitative analysis. *Br J Ophthalmol* 2003;87:1159–1166.
[46] Grunwald JE, Hariprasad SM, DuPont J, et al. Foveolar choroidal blood flow in age-related macular degeneration. *Invest Ophthalmol Vis Sci* 1998;39:385–390.
[47] Grunwald JE, Metelitsina TI, Dupont JC, Ying GS, Maguire MG. Reduced foveolar choroidal blood flow in eyes with increasing AMD severity. *Invest Ophthalmol Vis Sci* 2005;46:1033–1038.
[48] Ramrattan RS, van der Schaft TL, Mooy CM, et al. Morphometric analysis of Bruch's membrane, the choriocapillaris, and the choroid in aging. *Invest Ophthalmol Vis Sci* 1994;35:2857–2864.
[49] Sarks SH. Changes in the region of the choriocapillaries in aging and degeneration. Presented at the 23rd Concilium Ophthalmologicum, Kyoto, Japan. *Excerpta Medica Amsterdam* 1978;228–238.
[50] Sullivan R, Penfold P, Pow DV. Neuronal migration and glial remodeling in degenerating retinas of aged rats and in nonneovascular AMD. *Invest Ophthalmol Vis Sci* 2003;44:856–865.
[51] Wong J, Madigan M, Billson F, Penfold P. Quantification of leukocyte common antigen (CD45) expression in macular degeneration. Invest Ophthalmol Vis Sci 2001;42:*S227.*
[52] Cousins SW, Espinosa-Heidmann DG, Csaky KG. Monocyte activation in patients with age-related macular degeneration: a biomarker of risk for choroidal neovascularization? *Arch Ophthalmol* 2004;122:1013–1018.
[53] Ezzat MK, Hann CR, Vuk-Pavlovic S, Pulido JS. Immune cells in the human choroid. *Br J Ophthalmol* 2008;92:976–980.
[54] Cherepanoff S, McMenamin PG, Gillies MC, Kettle E, Sarks SH. Bruch's membrane and choroidal macrophages in early and advanced age-related macular degeneration. *Br J Ophthalmol.*2009.
[55] Espinosa-Heidmann DG, Suner IJ, Hernandez EP, et al. Macrophage depletion diminishes lesion size and severity in experimental choroidal neovascularization. *Invest Ophthalmol Vis Sci* 2003;44:3586–3592.
[56] Sakurai E, Anand A, Ambati BK, van Rooijen N, Ambati J. Macrophage depletion inhibits experimental choroidal neovascularization. *Invest Ophthalmol Vis Sci* 2003;44:3578–3585.
[57] Combadière C, Feumi C, Raoul W, et al. CX3CR1-dependent subretinal microglia cell accumulation is associated with cardinal features of age-related macular degeneration. *J Clin Invest* 2007;117:2920–2928.
[58] Dunaief JL, Dentchev T, Ying GS, Milam AH. The role of apoptosis in age-related macular degeneration. *Arch Ophthalmol* 2002;120:1435–1442.
[59] Sunness JS, Gonzalez-Baron J, Applegate CA, et al. Enlargement of atrophy and visual acuity loss in the geographic atrophy form of age-related macular degeneration. *Ophthalmology* 1999;106:1768–1779.
[60] Shelley EJ, Madigan MC, Natoli R, Penfold PL, Provis JM. Cone degeneration in aging and age-related macular degeneration. *Arch Ophthalmol* 2009;127:483–492.
[61] Rex TS, Fariss RN, Lewis GP, et al. A survey of molecular expression by photoreceptors after experimental retinal detachment. *Invest Ophthalmol Vis Sci* 2002;43:1234–1247.
[62] Bonilha VL, Hollyfield JG, Grover S, Fishman GA. Abnormal distribution of red/green cone opsins in a patient with an autosomal dominant cone dystrophy. *Ophthalmic Genet* 2005;26:69–76.
[63] John SK, Smith JE, Aguirre GD, Milam AH. Loss of cone molecular markers in rhodopsin-mutant human retinas with retinitis pigmentosa. *Mol Vis* 2000;6:204–215.
[64] Hageman GS, Luthert PJ, Victor Chong NH, et al. An integrated hypothesis that considers drusen as biomarkers of immune-mediated processes at the RPE-Bruch's membrane interface in aging and age-related macular degeneration. *Prog Retin Eye Res* 2001;20:705–732.
[65] Anderson DH, Mullins RF, Hageman GS, Johnson LV. A role for local inflammation in the formation of drusen in the aging eye. *Am J Ophthalmol* 2002;134:411–431.
[66] Nozaki M, Raisler BJ, Sakurai E, et al. Drusen complement components C3a and C5a promote choroidal neovascularization. *Proc Natl Acad Sci USA* 2006;103:2328–2333.
[67] Taylor HR, Muñoz B, West S, et al. Visible light and risk of age-related macular degeneration. *Trans Am Ophthalmol Soc* 1990;88:163–73; discussion 173.

[68] Taylor HR, West S, Muñoz B, et al. The long-term effects of visible light on the eye. *Arch Ophthalmol* 1992;110: 99–104.
[69] Fletcher AE, Bentham GC, Agnew M, et al. Sunlight exposure, antioxidants, and age-related macular degeneration. *Arch Ophthalmol* 2008;126:1396–1403.
[70] Cruickshanks KJ, Klein R, Klein BE, Nondahl DM. Sunlight and the 5-year incidence of early age-related maculopathy: the beaver dam eye study. *Arch Ophthalmol* 2001;119:246–250.
[71] Tomany SC, Cruickshanks KJ, Klein R, Klein BE, Knudtson MD. Sunlight and the 10-year incidence of age-related maculopathy: the Beaver Dam Eye Study. *Arch Ophthalmol* 2004;122:750–757.
[72] Mitchell P, Smith W, Wang JJ. Iris color, skin sun sensitivity, and age-related maculopathy. The Blue Mountains Eye Study. *Ophthalmology* 1998;105:1359–1363.
[73] Young RW. Solar radiation and age-related macular degeneration. *Surv Ophthalmol* 1988;32:252–269.
[74] Delcourt C, Carrière I, Ponton-Sanchez A, et al. POLA Study Group. Light exposure and the risk of age-related macular degeneration: the Pathologies Oculaires Liées à l'Age (POLA) study. *Arch Ophthalmol* 2001;119:1463–1468.
[75] Khan JC, Shahid H, Thurlby DA, et al. Genetic Factors in AMD Study. Age related macular degeneration and sun exposure, iris colour, and skin sensitivity to sunlight. *Br J Ophthalmol* 2006;90:29–32.
[76] West SK, Rosenthal FS, Bressler NM, et al. Exposure to sunlight and other risk factors for age-related macular degeneration. *Arch Ophthalmol* 1989;107:875–879.
[77] Hirakawa M, Tanaka M, Tanaka Y, et al. Age-related maculopathy and sunlight exposure evaluated by objective measurement. *Br J Ophthalmol* 2008;92:630–634.
[78] Klein R. Epidemiology of Age-related macular degeneration. In: Penfold P, Provis J (eds), *Macular Degeneration*. Berlin: Springer-Verlag, 2005.
[79] Organisciak DT, Darrow RM, Jiang YL, Blanks JC. Retinal light damage in rats with altered levels of rod outer segment docosahexaenoate. *Invest Ophthalmol Vis Sci* 1996;37: 2243–2257.
[80] Beatty S, Koh H, Phil M, Henson D, Boulton M. The role of oxidative stress in the pathogenesis of age-related macular degeneration. *Surv Ophthalmol* 2000;45:115–134.
[81] Winkler BS, Boulton ME, Gottsch JD, Sternberg P. Oxidative damage and age-related macular degeneration. *Mol Vis* 1999;5:32.
[82] Crabb JW, Miyagi M, Gu X, et al. Drusen proteome analysis: an approach to the etiology of age-related macular degeneration. *Proc Natl Acad Sci USA* 2002;99:14682–14687.
[83] Gu X, Meer SG, Miyagi M, et al. Carboxyethylpyrrole protein adducts and autoantibodies, biomarkers for age-related macular degeneration. *J Biol Chem* 2003;278:42027–42035.
[84] Gu J, Pauer GJ, Yue X, et al. Clinical Genomic and Proteomic AMD Study Group. Assessing susceptibility to age-related macular degeneration with proteomic and genomic biomarkers. *Mol Cell Proteomics* 2009;8:1338–1349.
[85] Hollyfield JG, Bonilha VL, Rayborn ME, et al. Oxidative damage-induced inflammation initiates age-related macular degeneration. *Nat Med* 2008;14:194–198.